Adaptive Control of Position Compensation for Cable-Conduit Mechanisms Used in Flexible Surgical Robots

T. N. Do[1], T. Tjahjowidodo[1], M. W. S. Lau[2] and S. J. Phee[1]

[1]*School of Mechanical and Aerospace Engineering, Nanyang Technological University, Robotic Research Centre, 50 Nanyang Avenue, Singapore, 639798, Singapore*

[2]*Newcastle University International Singapore (NUIS), 180 Ang Mo Kio Avenue 8, Block P, Room 220, Singapore 569830, Singapore*

Keywords: Surgical Robot, Cable-Conduit, Nonlinear Control, Adaptive Laws, Flexible Endoscope.

Abstract: Natural Orifice Transluminal Endoscopic Surgery (NOTES) is a method that allows for performing complex operations via natural orifices without skin incisions. Its main tool is a flexible endoscope. Cable-Conduit Mechanisms (CCMs) are often used in NOTES because of its simplicity, safety in design, and easy transmission. Backlash hysteresis nonlinearities between the cable and the conduit pose difficulties in the motion control of the NOTES system. It is challenging to achieve the precise position of robotic arms when the slave manipulator inside the humans body. This paper presents new approaches to model and control for pairs of CCMs. It is known that the change of cable-conduit configuration will affect the backlash hysteresis nonlinearities. To deal with such change, a new nonlinear and adaptive control scheme will be introduced. The backlash hysteresis parameters are online estimated under the assumption of availability of output feedback and unknown bound of nonlinear parameters. To validate the proposed approach, a prototype of single-DOF-Master-Slave system, which consists of a master console, a telesurgical workstation, and a slave manipulator, is also presented. The proposed compensation scheme is experimentally validated using the designed system. The results show that the proposed control scheme efficiently improves the tracking performances of the system regardless of the change of endoscope configuration.

1 INTRODUCTION

Flexible endoscope is used in minimally invasive surgery (MIS) to inspect and treat gastrointestinal (GI) tract disorders without making any abdominal incisions in the patients body (Zhang et al., 2014); (Ott et al., 2011); (Clark et al., 2012). One of the promising surgical procedures using flexible endoscopes is the natural orifice transluminal endoscopic surgery (NOTES). The flexible endoscope could reach potential surgical site via natural orifices or small incisions and perform flexible tasks with the attached robotic arms. A pair of Cable-Conduit Mechanisms (CCMs) or tendon-sheath mechanisms is often used to actuate the robotic joints inside the human body by controlling each of the degrees of freedom (DOFs) of the robotic arms. The CCM is preferred over other transmission systems because it can operate in restricted work spaces and in long, narrow, and tortuous paths. Compared with other mechanisms like cable-pulley or hyper-redundant mechanism, CCM offers high payload and greater flexibility. However, the main drawback in the CCM is the presence of nonlinear friction and backlash hysteresis. Control of precise motion of the robotic arms is prominently a challenging issue in the use of such mechanism. Recently, various models for the CCM have been proposed and discussed to enhance performances of the CCM. Many researchers (Kaneko et al., 1992); (Palli et al., 2012); (Sun et al., 2014); (Chiang et al., 2009); (Phee et al., 2010) used lumped mass model elements to characterize the tendon-sheath transmission. In other approaches, some authors (Agrawal et al., 2010b) proposed a set of partial differential equations to model the tendon-sheath nonlinearity using a number of tendon elements. However, limitations still exist. Firstly, if more elements of the CCM are taken into consideration to improve the accuracy, the computation becomes more complex. Secondly, a constant pretention for all tendon elements is assumed. Thirdly, the models need the information of sheath configuration along the endoscope. Lastly, discontinuous phenomena still exist in the model approaches due to the use of Coulomb friction model. Although Do and his col-

Do T., Tjahjowidodo T., Lau M. and Phee S..
Adaptive Control of Position Compensation for Cable-Conduit Mechanisms Used in Flexible Surgical Robots.
DOI: 10.5220/0005114701100117
In *Proceedings of the 11th International Conference on Informatics in Control, Automation and Robotics* (ICINCO-2014), pages 110-117
ISBN: 978-989-758-039-0

leagues (Do et al., 2013a), (Do et al., 2013b), (Do et al., 2014b), and (Do et al., 2014a) introduced novel dynamic friction model to overcome the discontinuity for estimated force feedback, no motion control schemes were introduced to compensate for the position errors.

It has been known that the backlash hysteresis profile varies with the endoscope configuration (Bardou et al., 2012),(Kesner and Howe, 2011), (Kesner and Howe, 2014). To achieve accurate tracking control, two approaches are usually considered. The first one is that feedback of the robotic joints is available and the closed-loop control is used. Online estimation of backlash hysteresis parameters with adaptive control laws is applied regardless of the changes of configuration. In this case, electromagnetic tracking system or image processing methods can be considered as a potential tool to provide the output feedback (Reilink et al., 2013). In the absence of the position feedback during the compensation, feedforward control scheme should be used. To improve the tracking performances using offline learning, a backlash hysteresis model and compensation control scheme with higher accuracy and degree of smoothness, and ease of implementation, are desired. For the design of backlash compensators, some researchers (Su et al., 2000); (Hu et al., 2013) used a very complex nonlinear and adaptive control algorithm to deal with the nonlinearities under the assumption of available output feedback. They indicated that the backlash model given by authors in (Tao and Kokotovic, 1995) is not suitable for the system control as the backlash function is discontinuous. Agrawal and his colleagues (Agrawal et al., 2010a) used a smooth inverse of backlash hysteresis model to compensate for the error. However, a smooth inverse model, a switching law for the velocity, and output feedback were needed. Do and his colleagues (Do et al., 2014c) used a direct inverse model-based feedforward to compensate for the position error in a single CCM. The compensator uses the direct inverse structure that does not require complex inversion of backlash hysteresis model and allows for easy implementations (Rakotondrabe, 2011); (Do et al., 2014c), (Hassani et al., 2014); (Minh et al., 2010), and (Vo-Minh et al., 2011). However, the change of cable-conduit mechanism has not been considered yet. To deal with this challenge, a direct control algorithm is developed regardless of the construction of inverse model (Cai et al., 2013); (Zhang et al., 2014). In this paper, new adaptive control laws are presented without using any inverse model for the compensation.

The control scheme in this paper allow for capturing the backlash hysteresis nonlinearities and efficacy of enhancing tracking performances regardless of the curvature and sheath angles. Compare to the other approaches (Agrawal et al., 2010a); (Bardou et al., 2012),(Kesner and Howe, 2011), (Kesner and Howe, 2014); (Do et al., 2014c), where the backlash hysteresis or the bound of parameters must be known in advance, in our schemes, their bounds are unknown and online estimated during the compensation. To validate the proposed approach, a dedicated single degree of freedom of a Master-Slave system is introduced. The system consists of a master console, actuator housing, and a slave manipulator. This type of system has been presented in NOTES systems like MASTER (Phee et al., 2010), (Abbott et al., 2007). Using the designed Master-Slave system, the proposed schemes are experimentally carried out to validate real surgical tasks such as gripping a determined object. The rests of this paper are organized as follow: In section 2, an overview of NOTES system and the transmission property of a pair of TSM are introduced. The design of the Master-Slave system for validation, which contains the master console, motor housing and slave manipulator, is introduced in this section. In addition, the development of nonlinear and adaptive control laws will be given. Experimental demonstration is presented in section 3. Finally, the conclusion is drawn in section 4.

2 MATERIALS AND METHODS

In order to evaluate the proposed control scheme, a human-subject platform is introduced. This section also presents the cable-conduit transmission characteristics and experimental instruments. Nonlinear and adaptive control laws for enhancing the tracking performance will be also given.

2.1 NOTES System and Cable-Conduit Characteristics

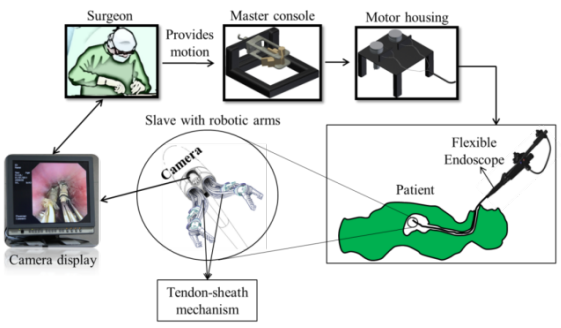

Figure 1: Overview of a NOTES system.

A typical Natural Orifice Transluminal Endoscopic Surgery (NOTES) system is illustrated in Fig. 1. Surgeons carry out the surgical tasks using a master console to control the slave manipulator (includes robotic arms) inside the patients body. The system consists of a master console, a slave manipulator, and a telesurgical workstation (motor housing). One of the main tools of NOTES is a long and flexible endoscope, i.e. a flexible shaft with an articulated bending tip and tool channels to house the robotic arms as well as a camera (provide visual feedback to the surgeon). The robotic arms which possess multiple degrees of freedom (DOFs) are fixed and carried along with the endoscope to perform demanding surgical procedures such as suturing and cutting. Triangulation is carried out at the distal end of the endoscope while actuation is externally provided.

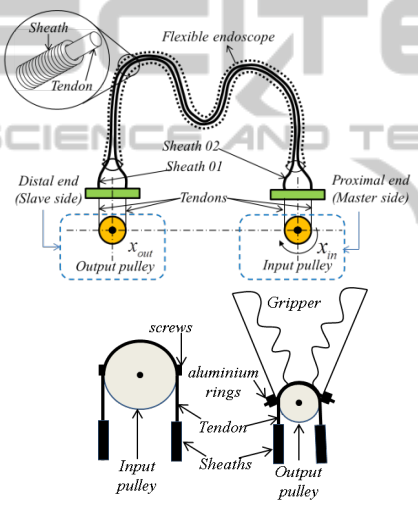

Figure 2: (Upper) Diagram for a pair of CCMs; (Lower) Ways for connecting cables (tendons) to pulleys.

To control each of the DOFs for the robotic arms, a pair of CCMs is often used. The pull-pull transmissions for the CCMs have been studied in (Kaneko et al., 1992); (Agrawal et al., 2010b). The upper panel of Fig. 2 shows the structure of a pair of the CCMs. x_{in} and x_{out} denote the displacements at the proximal end and at the distal end of the system, respectively. The two cables and conduits are routed along a flexible tube as the endoscope. Suppose that the input pulley initially rotates in the clockwise direction (positive velocity-see The upper panel of Fig. 2a). When the input pulley reverses its motion, the output pulley does not immediately rotate, which results in a certain delay. The tension decreases in the previously tensed cable. The loss of tensions along the conduit, which due to the gap and friction force between the cables and the conduits, results in delay for immediate transmission of motion from the input pulley (proximal end) to the output pulley (distal end). Once the friction between the cables and the conduit in the outer loop of the pair of CCMs is overcome, then the output pulley immediately rotates following the input pulley. Similar transmission characteristics are described for the reversal motion in counter-clockwise. This behavior of the transmission characteristics of the CCM is referred to as a backlash hysteresis profile. Note that the dead-band is not considered in this paper because the cables are always pre-tensed. From aforementioned descriptions, cable-conduit transmission can be approximately modeled as the backlash hysteresis where the nonlinear parameters of hysteresis profile depend on the cable-conduit configuration.

2.2 Experimental protocol

In this section, we introduce a dedicated experimental setup of a single-DOF Master-Slave system. The system consists of a master console, telesurgical workstation (include actuator housing and dSPACE controller), and a slave manipulator. For illustration, a slave system with a single-DOF robotic arm is considered. The overview of NOTES system has been illustrated in Fig. 1. The mechanism design of a

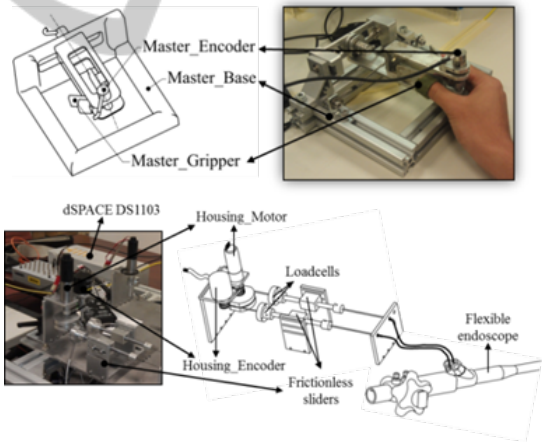

Figure 3: The master console and motor housing with diagrams and real photos:(Upper) Master console with two DOFs; (Lower) Actuator housing with two motors.

master console with a single-DOF, denoted as Master_Gripper is presented in The upper panel of Fig. 3a. The master console, which enables the user to control the robotic arm at the distal end, is an ergonomic human-machine interface. In the master console, one encoder (Master_Encoder) is mounted to the Master_Gripper to provide necessary signal (position-reference trajectory y_r) to the output pulley with an attached gripper. The encoder is type of SCA16 from SCANCON. Signal from the Mas-

ter_Encoder will be subsequently sent to the dSPCAE controller where the data are processed and the cables and conduits actuation are controlled. The users control the motions of a gripper mounted on the output pulley via Master_Gripper. The picture of the master console is shown in right side of the upper panel of Fig. 3. The telesurgical workstation (The lower

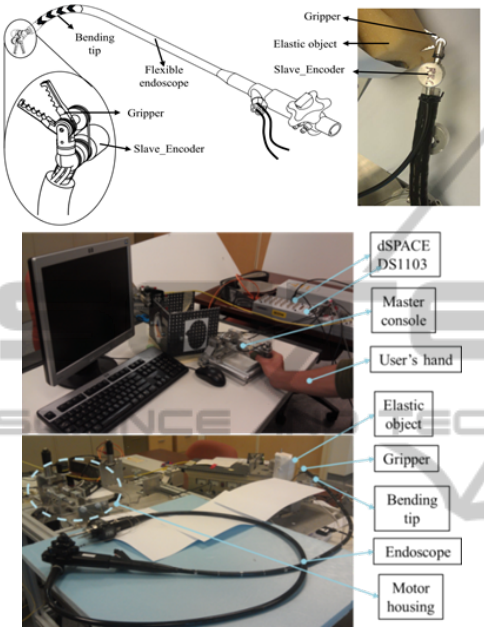

Figure 4: (Upper) Slave manipulator with two DOFs: (Lower) Photo of experimental setup.

panel of Fig. 3) consists of an actuator housing and dSPACE DS1103 controller. The controller consists of the control board, which is programmed via MATLAB Simulink from MathWorks. The signals from the master console and the robotic arm at distal end are also acquired to this system. The actuator housing includes a PITTMAN 8693 DC motors equipped with high resolution encoder E30. A input pulley, which actuates the slave joint (gripper with output pulley) using the CCMs, is also conneted to the motor. The CCMs are from Asahi Intecc Co. where the size of the cables is WR7x7D0.27mm with teflon coated wire ropes and the conduits with a round-wire coil and inner diameter of 0.36mm and outer diameter of 0.8mm. The length of the two conduits is 2 metre. The two CCMs are routed to follow a flexible endoscope and are connected to pulleys. At the input pulley, cables are fixed on the pulley using crews while at the output pulley, cables are fixed on corresponding holes using aluminium rings (see the lower panel of Fig. 2). In order to record the tensions at proximal end of the system, two load cells LW-1020-50 from Interface Corporation are used. They are mounted on frictionless sliders. The two cables and two conduits, subsequently, are used to actuate one of DOFs of the rotation joints. Noting that the tensions at proximal end are used to guarantee the same pretension when trials are repeated. Fig. 4 depicts the slave manipulator structure. In the experimental work, a gripper which is mounted on the tip of the endoscope is used as a robotic arm. The two cables are routed along two conduits passing through a flexible endoscope. The flexible endoscope, which is a type of GIF-2T160 from Olympus, Japan, has two tool channels with a length of 135cm. At each side (proximal end and distal end), the tendon is attached to corresponding pulleys (see the lower panel of Fig. 2). To measure the rotational displacement for the gripper joint at proximal end, a high resolution encoder Type SCA16 from SCANKON is utilized. The encoder is connected to the gripper joint via a small cable. The rotation motion of gripper is recorded by the dSPACE controller DS1103 via MATLAB environment from MathWorks.

2.3 Nonlinear and Adaptive Control

An adaptive control law is given in this section to deal with the change of cable-conduit configuration. If we consider this change as an unexpected disturbance, the nonlinear backlash hysteresis model which has been described in (Do et al., 2014c) can be rewritten by:

$$x_{out} = cu_{NL} + D \tag{1}$$

where D denotes the change of the hysteresis curve when the cable-conduit configuration varies, $u_{NL} = x_{in}$ represents for the control input, x_{out} is the output position.

Before going to the design of control law, some assumptions are made: (i) the cables are kept at some suitable pretension in order to avoid the cable slack, (ii) Output position feedback is used during the compensation, (iii) Uncertain parameter c is positive and its bound is unknown. Let the positive value D^* be the bound of which is assumed to be unknown. It will be estimated using the designed adaptive law; α is a positive parameter. Define a coordinate transformation ω and n for the system given by Eq. (1) and a tracking error e_r as follows:

$$\begin{cases} n = \int_0^t (y(\tau) - y_r(\tau))d\tau \\ e_r(t) = y(t) - y_r(t) \\ \omega = e_r(t) + \alpha \int_0^t e_r(\tau)d\tau = \dot{n} + \alpha n \end{cases} \tag{2}$$

The first order derivative of the new variable can

be expressed by:

$$\dot{\omega} = \alpha(y - y_r) + \dot{e}_r = \alpha(cu_{NL} + D - y_r) + \dot{e}_r \quad (3)$$

Denote the inverse of backlash hysteresis slope c by $\chi = 1/c$, then the estimate of χ and D^* will be stated as $\hat{\chi}$ and $\hat{D}^*$, respectively. Define $\tilde{D}^* = D^* - \hat{D}^*$ as the error estimate bound of disturbance D^*. From Eq. (2) and Eq. (3), the adaptive control law is designed as follows:

$$u_{NL} = -\hat{\chi}(k\omega + \text{sgn}(\omega)\hat{D}^* - y_r + (1/\alpha)\dot{e}_r) \quad (4)$$

$$\dot{\hat{\chi}} = \delta_1(k\omega + \text{sgn}\hat{D}^* - y_r + (1/\alpha)\dot{e}_r)\omega \quad (5)$$

$$\dot{\hat{D}}^* = \delta_2|\omega| \quad (6)$$

where k, δ_1, δ_2 are positive parameters that adjust the controller to force the tracking errors tend to compact sets.

With Eq. (3) to Eq. (6), the following theorem holds:

Theorem 1. *Consider the nonlinear system (Eq. 3) with uncertainties and satisfies the assumptions (i) to (iv). The following statements hold under the controller given by Eq. (4) and the update laws given by Eq. (5) and Eq. (6):*

1. *The closed loop system results in global stability.*
2. *The tracking errors e_r and estimates $\hat{\chi}, \hat{D}^*$ are uniformly ultimately bounded (UUB).*

Proof: We define the Lyapunov function V as follows:

$$V = 0.5\omega^2 + (0.5/\mu)(\tilde{D}^*)^2 + (c/2\delta)(\tilde{\chi})^2 \quad (7)$$

where $\tilde{\chi} = \chi - \hat{\chi}$ is error estimate of χ; μ, δ are positive parameters. The initial values of function V is $V(0) = 0.5(\omega(0))^2 + (0.5/\mu))(\tilde{D}^*(0))^2 + (c/2\delta)(\tilde{\chi}(0))^2$ with $\omega(0), \tilde{D}^*(0), \tilde{\chi}(0)$ are initial values of $\omega, \tilde{D}^*, \tilde{\chi}$, respectively.

The derivative of the Lyapunov function given by Eq. (7) can be obtained by:

$$\dot{V} = \omega\dot{\omega} - (1/\mu)\tilde{D}^*\dot{\hat{D}}^* - (c/\delta)\tilde{\chi}\dot{\hat{\chi}} = \omega(\alpha(cu_{NL} + D - y_r) + \dot{e}_r) - (1/\mu)\tilde{D}^*\dot{\hat{D}}^* - (c/\delta)\tilde{\chi}\dot{\hat{\chi}} \quad (8)$$

Note that the term u_{NL} can be expressed by:

$$cu_{NL} = c\hat{\chi}\bar{u} = c\hat{\chi}\bar{u} + \bar{u} - c\chi\bar{u} = \bar{u} - c\tilde{\chi}\bar{u} \quad (9)$$

where $\bar{u} = -k\omega - \text{sgn}(\omega)\hat{D}^* + y_r - (1/\alpha)\dot{e}_r$

Replace Eq. (4) to Eq. (6) into Eq. (8), one can obtain:

$$\begin{aligned}\dot{V} &= \omega(\alpha(cu_{NL} + D - y_r) + \dot{e}_r) - (1/\mu)\tilde{D}^*\dot{\hat{D}}^* \\ &- (c/\delta)\tilde{\chi}\dot{\hat{\chi}} = \omega(\alpha(-k\omega - \text{sgn}(\omega)\hat{D}^* + y_r - (1/\alpha)\dot{e}_r \\ &- c\tilde{\chi}\bar{u} + D - y_r) + \dot{e}_r) - (1/\mu)\tilde{D}^*\dot{\hat{D}}^* - (c/\delta)\tilde{\chi}\dot{\hat{\chi}} \\ &= -\alpha k\omega^2 - \alpha|\omega|\hat{D}^* + \alpha D\omega - (1/\mu)\tilde{D}^*\dot{\hat{D}}^* \\ &- (c/\delta)\tilde{\chi}(\alpha\delta\bar{u}\omega + \dot{\hat{\chi}}) = -\alpha k\omega^2 - (c/\delta)\tilde{\chi}(\alpha\delta\bar{u}\omega + \dot{\hat{\chi}}) \\ &+ (1/\mu)\tilde{D}^*(-\dot{\hat{D}}^* + \alpha\mu|\omega|) \leq -\alpha k\omega^2 \leq 0 \end{aligned} \quad (10)$$

where $\delta_1 = \alpha\delta, \delta_2 = \alpha\mu$

With the inequality given by Eq. (10), one can see that the Lyapunov function V is a decreasing function and bounded from below by zero. From Eq. (10), one can obtain $\dot{V} \leq 0 \iff V \leq V(0)$ where $V(0) = 0.5(\omega(0))^2 + (0.5/\mu)(\tilde{D}^*(0))^2 + (\alpha/2\rho)(\tilde{\chi}(0))^2 \geq 0$. Hence, variables $\omega, \tilde{D}^*, \tilde{\chi}$ are also bounded. From (7), one can obtain $0.5\omega^2 \leq V \leq V(0)$ or $|\omega| \leq \sqrt{2V(0)}$. Two cases for the solutions of n: Case(i) $\omega = \dot{n} + n\alpha \leq \sqrt{2V(0)}$ or $n \leq (n_0 - (1/\alpha)\sqrt{2V(0)})e^{-\alpha t} + (1/\alpha)\sqrt{2V(0)}$. There exists $t > T > 0$ such that $n \leq (1/\alpha)\sqrt{2V(0)}$ since $(n_0 - (1/\alpha)\sqrt{2V(0)})e^{-\alpha t} \to 0$ for any $t > T$. Case(ii) $\omega = \dot{n} + n\alpha \geq -\sqrt{2V(0)}$ or $n \geq (n_0 + (1/\alpha)\sqrt{2V(0)})e^{-\alpha t} - (1/\alpha)\sqrt{2V(0)}$. There exists $t > T > 0$ such that $n \geq -(1/\alpha)\sqrt{2V(0)}$ since $(n_0 + (1/\alpha)\sqrt{2V(0)})e^{-\alpha t} \to 0$ for any $t > T$. For both cases, we have:

$$|n| \leq (1/\alpha)\sqrt{2V(0)} \quad (11)$$

With $|\omega| \leq \sqrt{2V(0)}$ and (11), one can obtain:

$$\begin{aligned}|\dot{n}| - \alpha|n| \leq |\omega| = |\dot{n} + n\alpha| \leq \sqrt{2V(0)} \\ \text{or } |\dot{n}| \leq \alpha(1/\alpha)\sqrt{2V(0)} + \sqrt{2V(0)} \\ = 2\sqrt{2V(0)} \end{aligned} \quad (12)$$

Then, one can verify that the UUB tracking performance for the filter ω and its components $n, \dot{n} = e_r$ are guaranteed. It is also demonstrated that the update parameters are guaranteed to be UUB. The proof is completed here.

Remark 1: It is recommended that relevant validations based on simulation should be carried out before doing the practical experiments. Based on the simulation results, optimal parameters can be obtained.

3 REAL-TIME EXPERIMENTAL VALIDATIONS

For validation purpose, the motion of slave manipulation is investigated by random motions prescribed from the users movement through the master console. Fig. 5 illustrates the experimental setup and control schemes for validation test. In practical validation, the grasper is required to grip an elastic object that is controlled using the Master_Gripper (see Figs. 3, 4, and 5). A motion generated by the user via the master console is applied to the actuator housing at the proximal end (see Fig. 5). The Master_Encoder and Slave_Encoder are used to record the input and output motions at corresponding joints using the dSPACE

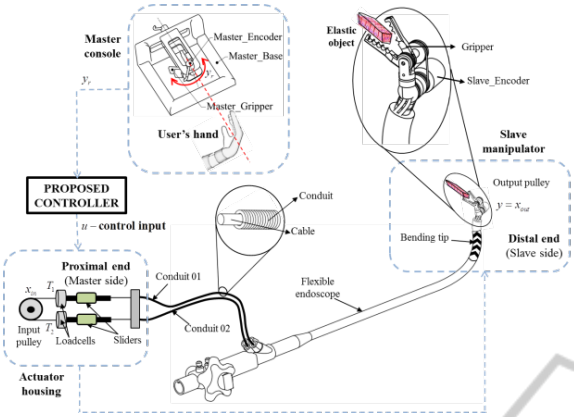

Figure 5: Compensation control structure for the Master-Slave system.

DS1103. The purpose is to control the output position y to follow a desired reference input y_r as close as possible.

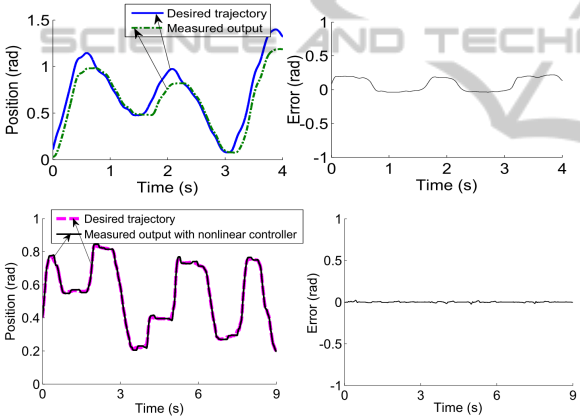

Figure 6: Compensation results: (Upper) Without compensation; (Lower) With nonlinear control; (Left) Position tracking; (Right) Tracking error.

Table 1: Quantitative measures for case of nonlinear and adaptive control.

Position (rad)		
Trials	Mean squared error	Standard deviation
1	0.000276	0.0166
2	0.000196	0.0140
3	0.000286	0.0169
4	0.000244	0.0156
5	0.000227	0.0159

In order to demonstrate the effectiveness of the proposed nonlinear adaptive scheme, a set of control parameters are established basing on relevant simulations, i.e. $k = 15, \alpha = 5, \delta_1 = 10, \delta_2 = 10$. The signum function is approximated using $\text{sgn}(\omega) = \omega/(|\omega| + 0.01)$ in order to avoid chattering during the implementation of the controller. The initial values for estimate variables are chosen to $\hat{\chi}(0) = 1$ and $\hat{D}^*(0) = 0$.

The experimental validations are carried out five times (five trials). For illustration purposes, one of the five trials will be given. Fig. 6 depicts the compensation results using nonlinear adaptive control scheme which is illustrated by the proposed structure in Fig. 5. In the case of no compensation control, the measured position output y always lags to the desired trajectory y_r. This phenomenon can be seen from the upper left panel of Fig. 6. When the nonlinear control scheme is used (see Fig. 5), the measured output y accurately follows the desired trajectory y_r (see the left panel of Fig. 6). The relative error under the nonlinear control scheme is also depicted in the right panel of Fig. 6. There is a significant reduction from 0.2669 rad peak-to-peak error before compensation to 0.08743 rad peak-to-peak after compensation. Quantitative measures of the results in terms of mean error and standard deviation for each of trials are shown in Table 1.

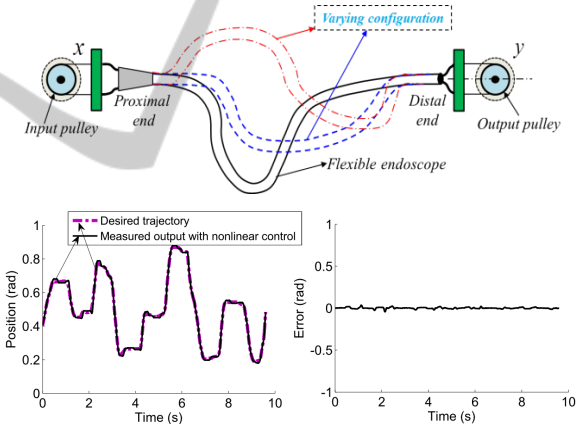

Figure 7: Compensation results with disturbance: (Upper) Random change of configuration; (Lower) Results for nonlinear control; (Left) Position tracking; (Right) Tracking error.

It is known that the backlash hysteresis profile will change if the configuration changes. Hence, the performances of proposed control scheme based on the change of endoscope configuration during the experiments are evaluated and discussed. The endoscope configuration, which is shown in the upper panel of Fig. 7, is varied during the experiments. When the nonlinear adaptive controller is applied (see the lower panel of Fig. 7), the phase lag and tracking error are almost around 0.09743 rad peak-to-peak. It can be concluded that the proposed control can adapt to any change of the endoscope configuration.

4 CONCLUSIONS

This paper introduces a new adaptive control scheme to enhance the tracking performances for a flexible endoscopic system using cable-conduit mechanisms. The proposed control laws are able to deal with nonlinearities in the presence of uncertainties and disturbances. Unlike current approaches of the cable-conduit control, our control scheme has efficiently reduced the tracking error and robustness. Experimental validations have been carried out using a real master-slave system to evaluate the controller performances. Comparisons between the proposed model and the experimental data show a good agreement. It has been demonstrated that the model approach works well on a real surgical device (Master-Slave system) in NOTES system to carry out the task of gripping a real object. It has also been indicated that the proposed scheme is able to track the desired reference signal regardless of the configuration of the endoscope. In addition, no knowledge of exact backlash hysteresis parameters is required. The proposed control scheme has opened potential benefits to other flexible endoscopic system for enhancing tracking performances of precise motion. Future activities will be conducted the validations for higher degrees of freedom of flexible endoscopic systems. In addition, in-vivo on live animal and human will be carried out for further validations.

REFERENCES

Abbott, D., Becke, C., Rothstein, R., and Peine, W. (2007). Design of an endoluminal notes robotic system. In *IEEE/RSJ International Conference on Intelligent Robots and Systems, IROS,*, pages 410–416.

Agrawal, V., Peine, W., Yao, B., and Choi, S. (2010a). Control of cable actuated devices using smooth backlash inverse. In *IEEE International Conference on Robotics and Automation (ICRA)*, pages 1074–1079. Anchorage, AK.

Agrawal, V., Peine, W. J., and Yao, B. (2010b). Modeling of transmission characteristics across a cable-conduit system. *IEEE Transactions on Robotics*, 26(5):914–924.

Bardou, B., Nageotte, F., Zanne, P., and De Mathelin, M. (2012). Improvements in the control of a flexible endoscopic system. In *IEEE International Conference on Robotics and Automation (ICRA)*, pages 3725–3732. Saint Paul, MN.

Cai, J., Wen, C., Su, H., and Liu, Z. (2013). Robust adaptive failure compensation of hysteretic actuators for a class of uncertain nonlinear systems. *IEEE Transactions on Automatic Control*, 58(9):2388–2394.

Chiang, L. S., Jay, P. S., Valdastri, P., Menciassi, A., and Dario, P. (2009). Tendon sheath analysis for estimation of distal end force and elongation. In *IEEE/ASME International Conference on Advanced Intelligent Mechatronics (AIM)*, pages 332–337.

Clark, M. P., Qayed, E. S., Kooby, D. A., Maithel, S. K., and Willingham, F. F. (2012). Natural orifice translumenal endoscopic surgery in humans: a review. *Minimally invasive surgery*, 2012.

Do, T. N., Tjahjowidodo, T., Lau, M. W. S., and Phee, S. J. (2013a). Dynamic friction model for tendon-sheath actuated surgical robots: modelling and stability analysis. In *ISRM 2013-Proceedings of the 3rd International Symposium on Robotics and Mechatronics*, pages 302–311. Singapore.

Do, T. N., Tjahjowidodo, T., Lau, M. W. S., and Phee, S. J. (2013b). Nonlinear modeling and parameter identification of dynamic friction model in tendon sheath for flexible endoscopic systems. In *ICINCO 2013-Proceedings of the 10th International Conference on Informatics in Control, Automation and Robotics*, pages 5–10. Reykjavik, Iceland.

Do, T. N., Tjahjowidodo, T., Lau, M. W. S., and Phee, S. J. (2014a). Dynamic friction-based force feedback for tendon-sheath mechanism in notes system. *International Journal of Computer and Electrical Engineering*, 6(3):252–258.

Do, T. N., Tjahjowidodo, T., Lau, M. W. S., and Phee, S. J. (2014b). An investigation of friction-based tendon sheath model appropriate for control purposes. *Mechanical Systems and Signal Processing*, 42(1-2):97–114.

Do, T. N., Tjahjowidodo, T., Lau, M. W. S., Yamamoto, T., and Phee, S. J. (2014c). Hysteresis modeling and position control of tendon-sheath mechanism in flexible endoscopic systems. *Mechatronics*, 24(1):12 – 22.

Hassani, V., Tjahjowidodo, T., and Do, T. N. (2014). A survey on hysteresis modeling, identification and control. *Mechanical Systems and Signal Processing*, 49(1):209–233.

Hu, C., Yao, B., and Wang, Q. (2013). Performance-oriented adaptive robust control of a class of nonlinear systems preceded by unknown dead zone with comparative experimental results. *IEEE/ASME Transactions on Mechatronics*, 18(1):178–189.

Kaneko, M., Paetsch, W., and Tolle, H. (1992). Input-dependent stability of joint torque control of tendon-driven robot hands. *IEEE Transactions on Industrial Electronics*, 39(2):96–104.

Kesner, S. and Howe, R. (2011). Position control of motion compensation cardiac catheters. *IEEE Transactions on Robotics*, 27(6):1045–1055.

Kesner, S. B. and Howe, R. D. (2014). Robotic catheter cardiac ablation combining ultrasound guidance and force control. *The International Journal of Robotics Research*, 33(4):631–644.

Minh, T. V., Kamers, B., Tjahjowidodo, T., Ramon, H., and Van Brussel, H. (2010). Modeling torque-angle hysteresis in a pneumatic muscle manipulator. In *IEEE/ASME International Conference on Advanced Intelligent Mechatronics (AIM)*, pages 1122–1127.

Ott, L., Nageotte, F., Zanne, P., and de Mathelin, M. (2011). Robotic assistance to flexible endoscopy by physiological-motion tracking. *IEEE Transactions on Robotics*, 27(2):346–359.

Palli, G., Borghesan, G., and Melchiorri, C. (2012). Modeling, identification, and control of tendon-based actuation systems. *IEEE Transactions on Robotics*, 28(2):277–290.

Phee, S. J., Low, S., Dario, P., and Menciassi, A. (2010). Tendon sheath analysis for estimation of distal end force and elongation for sensorless distal end. *Robotica*, 28(07):1073–1082.

Rakotondrabe, M. (2011). Bouc-wen modeling and inverse multiplicative structure to compensate hysteresis nonlinearity in piezoelectric actuators. *IEEE Transactions on Automation Science and Engineering*, 8(2):428–431.

Reilink, R., Stramigioli, S., and Misra, S. (2013). Image-based hysteresis reduction for the control of flexible endoscopic instruments. *Mechatronics*, 23(6):652–658.

Su, C.-Y., Stepanenko, Y., Svoboda, J., and Leung, T. (2000). Robust adaptive control of a class of nonlinear systems with unknown backlash-like hysteresis. *IEEE Transactions on Automatic Control*, 45(12):2427–2432.

Sun, Z., Wang, Z., and Phee, S. J. (2014). Elongation modeling and compensation for the flexible tendon–sheath system. *IEEE/ASME Transactions on Mechatronics*, 19(4):1243–1250.

Tao, G. and Kokotovic, P. (1995). Adaptive control of system with unknown output backlash. *IEEE Transactions on Automatic Control*, 40(2):326–330.

Vo-Minh, T., Tjahjowidodo, T., Ramon, H., and Van Brussel, H. (2011). A new approach to modeling hysteresis in a pneumatic artificial muscle using the maxwell-slip model. *IEEE/ASME Transactions on Mechatronics*, 16(1):177–186.

Zhang, Z., Xu, S., and Zhang, B. (2014). Asymptotic tracking control of uncertain nonlinear systems with unknown actuator nonlinearity. *IEEE Transactions on Automatic Control*, 59(5):1336–1341.